ORIGINAL ARTICLE

Widespread corticopetal projections from the oval paracentral nucleus of the intralaminar thalamic nuclei conveying orofacial proprioception in rats

Yumi Tsutsumi[1] · Yuka Mizuno[1,2] · Tahsinul Haque[1,6] · Fumihiko Sato[1] · Takahiro Furuta[1] · Ayaka Oka[2] · Masayuki Moritani[3] · Yong Chul Bae[4] · Takashi Yamashiro[2] · Yoshihisa Tachibana[5] · Atsushi Yoshida[1]

Abstract

The oval paracentral nucleus (OPC) was initially isolated from the paracentral nucleus (PC) within the intralaminar thalamic nuclei in rats. We have recently shown that the rat OPC receives proprioceptive inputs from jaw-closing muscle spindles (JCMSs). However, it remains unknown which cortical areas receive thalamic inputs from the OPC, and whether the cortical areas receiving the OPC inputs are distinct from those receiving inputs from the other intralaminar nuclei and sensory thalamic nuclei. To address this issue, we injected an anterograde tracer, biotinylated dextranamine (BDA), into the OPC, which was electrophysiologically identified by recording of proprioceptive inputs from the JCMSs. Many BDA-labeled axonal fibers and terminals from the OPC were ipsilaterally observed in the rostral and rostroventral regions of the primary somatosensory cortex (S1), the rostral region of the secondary somatosensory cortex (S2), and the most rostrocaudal levels of the granular insular cortex (GI). In contrast, a BDA injection into the caudal PC, which was located slightly rostral to the OPC, resulted in ipsilateral labeling of axonal fibers and terminals in the rostrolateral region of the medial agranular cortex and the rostromedial region of the lateral agranular cortex. Furthermore, injections of a retrograde tracer, Fluorogold, into these S1, S2, and GI regions, resulted in preferential labeling of neurons in the ipsilateral OPC among the intralaminar and sensory thalamic nuclei. These findings reveal that the rat OPC has widespread, but strong corticopetal projections, indicating that there exist divergent corticopetal pathways from the intralaminar thalamic nucleus, which process JCMS proprioceptive sensation.

Keywords Thalamus · OPC · Deep sensation · Muscle sensation · Cerebral cortex

Abbreviations

5C	Trigeminal sensory nucleus caudalis
5I	Trigeminal sensory nucleus interpolaris
12	Hypoglossal nucleus

Yumi Tsutsumi and Yuka Mizuno equally contribute to this study.

✉ Yoshihisa Tachibana
yoshi@med.kobe-u.ac.jp

✉ Atsushi Yoshida
yoshida@dent.osaka-u.ac.jp

[1] Department of Oral Anatomy and Neurobiology, Osaka University Graduate School of Dentistry, Suita, Osaka 565-0871, Japan

[2] Department of Orthodontics and Dentofacial Orthopedics, Osaka University Graduate School of Dentistry, Suita, Osaka 565-0871, Japan

[3] Department of Physical Therapy, Faculty of Health Science, Morinomiya University of Medical Sciences, Osaka 559-8611, Japan

[4] Department of Anatomy and Neurobiology, School of Dentistry, Kyungpook National University, Daegu 700-412, Korea

[5] Division of System Neuroscience, Kobe University Graduate School of Medicine, Kobe, Hyogo 650-0017, Japan

[6] Present Address: Department of Oral Medicine and Diagnostic Sciences, College of Dentistry, King Saud University, Riyadh 11545, Saudi Arabia

ABC	Avidin–biotin-peroxidase complex
ac	Anterior commissure
Acb	Accumbens nucleus
AcbC	Core part of the Acb
AcbS	Shell part of the Acb
ACg	Anterior cingulate cortex
Agl	Lateral agranular cortex
Agm	Medial agranular cortex
AI	Agranular insular cortex
BDA	Biotinylated dextranamine
cc	Corpus callosum
CeA	Central amygdaloid nucleus
Cl	Claustrum
CL	Centrolateral thalamic nucleus
CM	Central medial thalamic nucleus
CPu	Caudate putamen
Cu	Cuneate nucleus
DAB	Diaminobenzidine
dGIrvs2	Dorsal part of GI rostroventrally adjacent to the rostralmost part of S2
DI	Dysgranular insular cortex
DLO	Dorsolateral orbital cortex
DP	Dorsal peduncular cortex
ECu	External cuneate nucleus
FG	Fluorogold
fr	Fasciculus retroflexus
GI	Granular insular cortex
ic	Internal capsule
IL	Infralimbic cortex
IPAC	Interstitial nucleus of the posterior limb of the anterior commissure
JCMS	Jaw-closing muscle spindle
LGP	Lateral globus pallidus
LO	Lateral orbital cortex
MD	Mediodorsal thalamic nucleus
Me5	Trigeminal mesencephalic nucleus
ml	Medial lemniscus
MO	Medial orbital cortex
Mo5	Trigeminal motor nucleus
mt	Mammillothalamic tract
OPC	Oval paracentral thalamic nucleus
Or	Orbital cortex
Pb	Parabrachial nucleus
PB	Phosphate buffer
PBS	Phosphate-buffered saline
PC	Paracentral thalamic nucleus
PF	Parafascicular thalamic nucleus
Pom	Medial part of posterior thalamic complex
PrL	Prelimbic cortex
RF	Rhinal fissure
Rt	Reticular thalamic nucleus
S1	Primary somatosensory cortex
S2	Secondary somatosensory cortex

sm	Stria medullaris of the thalamus
Sm	Submedial thalamic nucleus
Sol	Solitary tract nucleus
Su5	Supratrigeminal nucleus
TSNC	Trigeminal sensory nuclear complex
Va	Outer part of layer V
VA	Ventral anterior thalamic nucleus
Vb	Inner part of layer V
VL	Ventrolateral thalamic nucleus
VM	Ventromedial thalamic nucleus
VO	Ventral orbital cortex
VPL	Ventral posterolateral thalamic nucleus
VPLo	Oral region of the VPL
VPM	Ventral posteromedial thalamic nucleus
VPMcvm	Caudo-ventromedial edge of the VPM
VPPC	Parvicellular part of the ventral posterior thalamic nucleus

Introduction

Multiple corticopetal pathways convey orofacial sensations (Fig. 1). These include the pathway that projects from the trigeminal ganglion neuron–trigeminal sensory nuclear complex–core part of the ventral posteromedial thalamic nucleus (VPM)–primary and secondary somatosensory cortices (S1 and S2), as well as the pathway that projects from the trigeminal ganglion neuron–trigeminal sensory nuclear complex–medial part of the posterior thalamic complex (Pom)–predominantly to the S2 rather than the S1 (pale-green routes in Fig. 1) (Dubner et al. 1978; Waite and Tracey 1985; Waite 2004; Jones 2007). Both pathways are known to convey orofacial sensations including cutaneous/mucosal sensations and deep sensations, but exclude the proprioception arising from jaw-closing muscle spindles (JCMSs) (Dubner et al. 1978; Lund et al. 1978). Orofacial nociception and thermal sensation are also conveyed through a third circuit: the trigeminal ganglion neuron–trigeminal sensory nucleus interpolaris/nucleus caudalis–submedial thalamic nucleus (Sm)–ventrolateral orbital cortex pathway (pale-purple routes in Fig. 1) (Dostrovsky et al. 1987; Dostrovsky and Guilbaud 1988; Yoshida et al. 1991, 1992; Ikeda et al. 2003). The fourth orofacial corticopetal route is the taste pathway, through which signals travel via the solitary tract nucleus–parabrachial nucleus–parvicellular part of the ventral posterior thalamic nucleus (VPPC, so-called gustatory thalamus)–dysgranular insular cortex (DI) (pale-gray route in Fig. 1) (Hamilton and Norgren 1984; Kosar et al. 1986; Herbert et al. 1990; Allen et al. 1991; Nakashima et al. 2000). These earlier studies indicate that the corticopetal pathways are well organized depending on the respective sensory modalities.

Fig. 1 Summary diagram showing multiple corticopetal pathways ▶ which convey orofacial sensations based on previous studies. There exist several ascending projections: orofacial cutaneous/mucosal sensations (pale-green routes), orofacial nociception and thermal sensation (pale-purple route), taste (pale-gray route), and proprioception arising from jaw-closing muscle spindles (JCMSs) (thin red routes). In terms of JCMS proprioception, we have recently reported on two pathways to the thalamus: (1) the JCMS–supratrigeminal nucleus (Su5)–caudo-ventromedial edge (VPMcvm) of the ventral posteromedial thalamic nucleus (VPM) pathway, and (2) the JCMS–Su5–oval paracentral thalamic nucleus (OPC) pathway. We have further reported that the VPMcvm projects to the dorsal part (dGIrvs2) of the granular insular cortex (GI) rostroventrally adjacent to the rostralmost part of the secondary somatosensory cortex (S2). The goal of this study was to investigate corticopetal projections from the OPC (thick red route) and paracentral thalamic nucleus (PC) (thick blue route). For explanations regarding the other pathways, see the Introduction section in the main text. To facilitate understanding of the entire ascending system, only the trigeminal sensory nucleus interpolaris (5I)/nucleus caudalis (5C)–contralateral side of the submedial thalamic nucleus (Sm) pathway, the solitary tract nucleus (Sol)–ipsilateral side of the parabrachial nucleus (Pb) pathway, the Pb–contralateral side of the parvicellular part of the ventral posterior thalamic nucleus (VPPC) pathway, the Su5–contralateral side of the VPMcvm pathway, and the Su5–contralateral side of the OPC pathway are shown, although these pathways are actually bilateral. For abbreviations, see the abbreviations list

With respect to the proprioceptive sensation, the proprioceptive inputs from the body have been considered to be conveyed to the "rostrodorsal shell" or rostral (oral) region (VPLo) of the ventral posterolateral thalamic nucleus (VPL) in several animal species (monkey, Friedman and Jones 1981; Maendly et al. 1981; Jones and Friedman 1982; Jones et al. 1982; cat, Andersson et al. 1966; rat, Francis et al. 2008). Therefore, the orofacial proprioceptive sensation had been thought to be processed in the "rostrodorsal shell" of the VPM (medially adjacent to the VPLo) (Jones and Friedman 1982). However, we have demonstrated that the rat JCMS proprioceptive inputs are conveyed to the supratrigeminal nucleus (Su5) by primary afferent neurons in the trigeminal mesencephalic nucleus (Fujio et al. 2016), and, then, to two different thalamic nuclei: prominently to the "caudo-ventromedial edge" (VPMcvm) of the VPM and moderately to the oval paracentral thalamic nucleus (OPC) in the intermedullary lamina (Yoshida et al. 2017; Sato et al. 2020) (thin red route in Fig. 1). Importantly, both the VPMcvm and the OPC were spatially distant from the "rostrodorsal shell" of the VPM described above (Yoshida et al. 2017; Sato et al. 2020). In addition, our recent study (Uemura et al. 2020) has demonstrated that the rat external cuneate nucleus, which receives proprioceptive inputs from forelimb and neck muscles, sends projections to the "ventromedial part" of the VPL adjacent to the VPMcvm, but not to the "rostrodorsal shell" of the VPL. These reports suggest that the thalamic relay of the proprioceptive sensation in rats may be located outside the classically considered
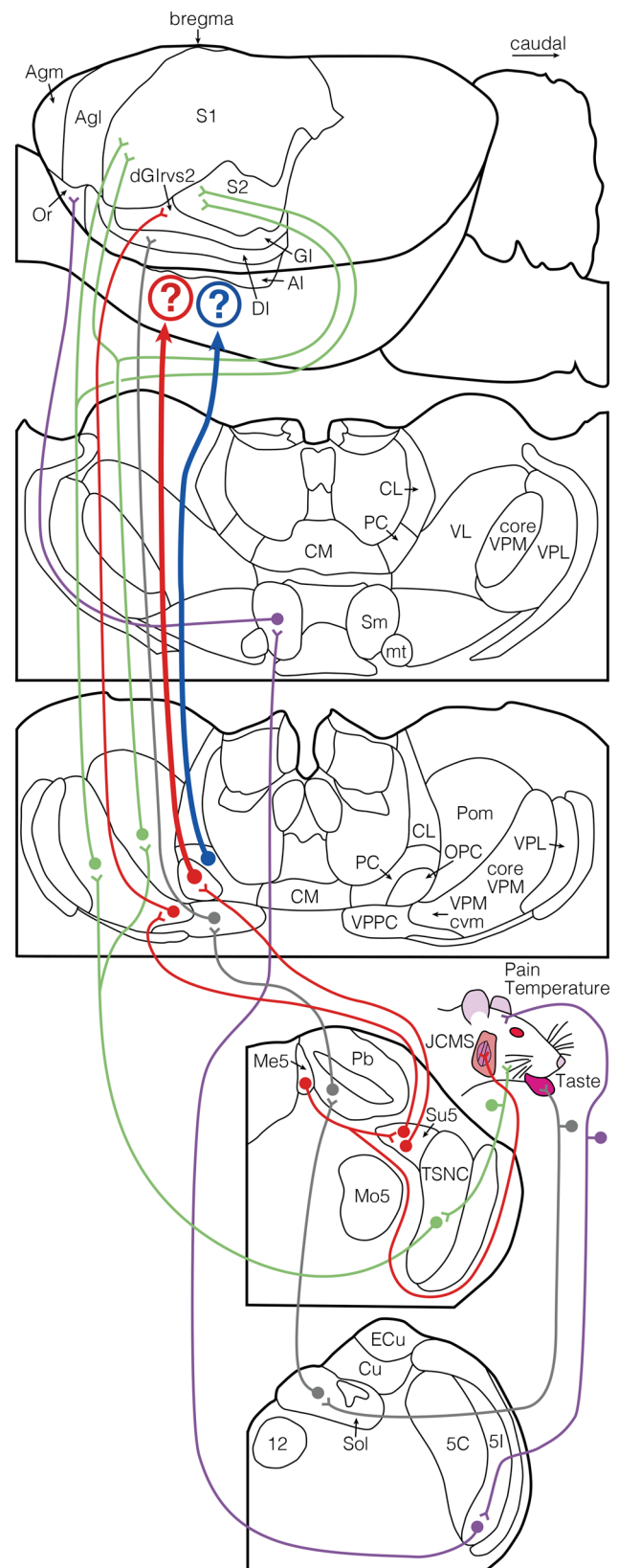
thalamocortical "rostrodorsal VPL/rostrodorsal VPM"–S1 pathway. Thus, it is essential to examine the corticopetal projections from the rat VPMcvm, OPC, and "ventromedial part" of the VPL to fully understand the central processing of the proprioceptive sensation. Consistent with this scenario, we have already demonstrated that the JCMS proprioceptive sensation via the VPMcvm is conveyed mostly to the dorsal part (dGIrvs2) of the granular insular cortex (GI) rostroventrally adjacent to the rostral-most part of the S2 (the trigeminal mesencephalic nucleus neuron–Su5–VPMcvm–dGIrvs2 route is denoted with thin red route in Fig. 1). However, the JCMS proprioceptive sensation via the VPMcvm hardly projected to the S1 and S2, and never to motor cortical areas (Sato et al. 2017). This is in contrast to previous findings that the proprioceptive sensation arising from body muscles including orofacial muscles can be recorded in area 3a of the S1 in humans, monkeys, and cats (e.g. Amassian and Berlin 1958; Phillips et al. 1971; Lund and Sessle 1974; Sirisko and Sessle 1983; Gandevia and Macefield 1989; Macefield et al. 1989). These earlier findings raise the possibility that, instead of the VPMcvm, the rat OPC conveys the proprioceptive sensation to the S1 that corresponds to the area 3a in other animal species.

Among the above-mentioned thalamic relay nuclei conveying orofacial sensations, the OPC is only the structure located in the intralaminar thalamic nuclei. The OPC was initially identified in the rat atlas by Paxinos and Watson (1986) as an ovoid region in the caudal level of the paracentral thalamic nucleus (PC) in the intermedullary lamina. The intralaminar thalamic nuclei generally receive projections from motor-related structures, such as the substantia nigra and the cerebellum, and send projections to the striatum and the motor cortical areas [the lateral agranular cortex (Agl) and the medial agranular cortex (Agm)] (Haroian et al. 1981; Berendse and Groenewegen 1991; Groenewegen et al. 1999; Jones 2007; Iwai et al. 2015). These findings suggest the possibility that the rat OPC projects not only to the S1 but also to the motor cortices. Therefore, the present study was aimed to reveal corticopetal pathways that originate from the OPC and possibly convey JCMS proprioceptive sensation (thick red route in Fig. 1) by means of anterograde and retrograde neuronal tract-tracing methods.

We also sought to compare the detailed features of thalamocortical projection from the OPC with those from the other sensory thalamic relay nuclei (core VPM, Pom, Sm, and VPPC) and the other intralaminal thalamic nuclei [the centrolateral nucleus (CL), PC, central medial nucleus (CM), and parafascicular nucleus (PF)]. Although Berendse and Groenewegen (1991) and Van der Werf et al. (2002) have already described the detailed features of corticopetal projections from the intralaminal thalamic nuclei in rats, they did not distinguish the OPC from the caudal PC. In the

present study, therefore, we have also examined the features of corticopetal projections from the caudal PC only (thick blue route in Fig. 1).

Materials and methods

Animals and tracer injections

The experiments described here were performed on 36 male Wistar rats weighing 250–330 g. All experimental procedures were approved by the animal ethics committees of the Osaka University Graduate School of Dentistry for the care and use of laboratory animals, and the experiment was performed in accordance with the relevant guidelines. Efforts were made to minimize animal suffering and the number of animals used. All animals used were anesthetized by intraperitoneal administration (i.p.) of ketamine hydrochloride (90 mg/kg) and xylazine hydrochloride (10 mg/kg) dissolved in saline, with supplementary doses given such that neither spontaneous eye movements nor corneal reflexes were apparent. A local injection of lidocaine hydrochloride was administered before making a skin incision if necessary. The rectal temperature was maintained between 37 and 38 °C with a heating pad, and electrocardiography was performed continuously. Rat brain atlases published by Paxinos and Watson (1998, 2014) were primarily used to determine the coordinates for stereotaxic micropipette insertion.

We aimed to extracellularly inject an anterograde tracer into the OPC (in the first experiment) and the caudal PC (in the second experiment) to label the axonal tract (fibers) and axonal terminals distributing in the cerebral cortex. To this end, an incision was made in the buccal skin to expose the masseter muscle on the right side, and the masseter nerve (which innervates JCMSs) was dissected so that it was free from the surrounding masseter muscle. Then, silver bipolar stimulation hook electrodes were positioned on the masseter nerve to enable electrical stimulation (single pulse, 200-μs duration, one–tenfold greater than the threshold for evoking the jaw-opening reflex, 1 Hz). After the initial surgery, the animal's head was placed in a stereotaxic apparatus. The left parietal bone was partly removed and a small portion of dura was incised to allow the vertical insertion of a glass micropipette filled with 2.0 M potassium citrate into the OPC. The glass electrode was inserted to target the center of the OPC (approximately 1.3 mm lateral, 3.6 mm caudal, and 6.6 mm ventral to the bregma) by reference to the rat brain atlas. Then, the exact location of the OPC was identified by monitoring of field potentials in response to electrical stimulation of the contralateral masseter nerve, as well as by unit recordings of responses to passive, sustained jaw-opening movements, in accordance with the electrophysiological criteria established in our previous study (Sato et al.

2020). For the sustained jaw-opening movements (muscle stretches), the mandible was manually depressed using a hand-held plastic probe inserted into the mouth. Following electrophysiological identification of the OPC, the glass micropipette was changed to a micropipette filled with an anterograde tracer [4% of biotinylated dextranamine (BDA; 10 K MW, Molecular Probes, Eugene, OR, USA) dissolved in saline] and reinserted the micropipette into the OPC in a similar manner. We employed BDA with high MW (10 K), because it is the most popularly used neuronal tracer for excellent anterograde tract-tracing (for reviews, see Lanciego and Wouterlood 2011; Wouterlood 2015). Then, BDA was extracellularly injected in an electrophoretic manner by delivering 2.0-µA positive pulses (300-ms duration, 2 Hz) for 5–7 min into the identified OPC. In the second experiment, we extracellularly injected BDA into the caudal PC by shifting the position of the electrode 0.2–0.3 mm dorsally and 0.4–0.6 mm rostrally with respect to the identified OPC in the first experiment.

In the third experiment, we made extracellular injections of a retrograde tracer into the cerebral cortical areas where the BDA-labeled axon terminals were found in the first experiment. This procedure allowed us to identify thalamic neurons of origin of projections to the cerebral cortices. To this end, we used Fluorogold (FG, Fluorochrome, Englewood, CO, USA), because it is the most frequently used neuronal tracer for excellent retrograde tract-tracing (for reviews, see Lanciego and Wouterlood 2011; Wouterlood 2015). After fixing the animal's head in a stereotaxic apparatus, we incised the left parietal skin, partly removed the parietal bone, and cut the dura mater on the cortical surface. Then, using stereotaxic methods, we vertically inserted a glass microelectrode filled with 1% FG dissolved in saline into the cortical areas, and electrophoretically injected FG for 10–20 min with 2.0-µA positive pulses (300-ms duration, 2 Hz). The exact locations of BDA and FG injection sites were later confirmed histologically.

After the tracer injections in all of the experiments, the glass microelectrode was withdrawn from the brain. (In the first and second experiments, the hook electrodes were detached from the masseter nerve.) All wounds were sutured, and an antibiotic (cefotiam hydrochloride, 66 mg/kg) and an analgesic (flurbiprofen axetil, 3.3 mg/kg) were administered (i.p.).

Histology

Five to seven days after the tracer injections, all rats were deeply anesthetized with an overdose of sodium pentobarbital (100 mg/kg, i.p.) and then perfused transcardially with 0.02 M phosphate-buffered saline (PBS, pH 7.4) followed by a fixative solution of 4% paraformaldehyde in 0.1 M phosphate buffer (PB, pH 7.4). The brain was removed

and cryoprotected in 20% sucrose dissolved in 0.02 M PB. Serial 60-µm coronal sections were then cut on a freezing microtome and successively divided into three sets.

For visualization of BDA in the first and second experiments, all sets of sections were incubated in 0.02 M PBS containing avidin–biotin-peroxidase complex (ABC) diluted to 1:100, and then reacted in diaminobenzidine (DAB) solution [0.1 M PB (pH 7.4) containing 0.04% DAB, 0.08% nickel ammonium sulfate, and 0.006% H_2O_2]. In the rats injected with FG in the third experiment, one set of sections was processed without any subsequent reactions. The remaining two sets of sections were incubated in 0.02 M PBS containing 3% normal goat serum, 0.2% Triton X-100, and a polyclonal rabbit anti-FG primary antibody (Chemicon, CA, USA: product No. AB153) diluted to 1:10,000. The sections were incubated in 0.02 M PBS containing biotinylated goat anti-rabbit immunoglobulin G diluted to 1:400, and then in 0.02 M PBS containing ABC diluted to 1:100. Subsequently, the sections were incubated in the DAB solution. In control experiments where FG was not injected or the primary antibody was omitted, no labeling was detected. Finally, all sections were mounted on gelatin-coated slides and dried, and one set of sections in each experiment was counterstained with Neutral red or Thionin. All sections were dehydrated in a graded alcohol series, cleared in limonene, and coverslipped.

Data analysis

Recorded field potentials were digitally stored, and offline analysis was performed using PowerLab 8/30 (ADInstruments, Sydney, Australia). Responses to five to ten successive electrical stimulations of the masseter nerve were averaged at each recording site.

We tried to count the number of anterogradely BDA-labeled axonal boutons (both en passant boutons and terminal boutons) in long strip-shaped areas (with 200-µm wide), which were aligned orthogonal to the pial surface of the cerebral cortex, by reference to the method employed in earlier studies (Krettek and Price 1977a, b). We first draw the labeled boutons identified in non-counterstained sections under a light microscope (60× oil immersion objective lens) with the camera-lucida as in our previous studies (Yoshida et al. 2001, 2005). Spatial position of each bouton in a particular layer of specific cortical areas was determined on the basis of the cytoarchitectonically delineated cortical areas and layers of the neighboring counterstained sections. Then, we counted the labeled boutons in each cortical area.

To obtain the lateral views of the distribution of anterogradely BDA-labeled axons and of FG injection sites in the cerebral cortex as in our previous studies (Sato et al. 2017; Ikenoue et al. 2018; Tsutsumi et al. 2018), we first draw the distribution of these labels found in non-counterstained

sections under a light microscope (10× or 20× objective lens) with a camera-lucida. We, then, depicted the distribution of the anterograde labeling in an orthogonal direction to the pial surface of the cerebral cortex on the camera-lucida drawings. We judged the position of the distribution of the depicted labels on the basis of the cytoarchitectonically delineated cortical areas of the neighboring counterstained sections.

In addition, as in our previous studies (Chang et al. 2009; Iida et al. 2010), we tried to count the number of retrogradely FG-labeled neuronal cell bodies in each thalamic nucleus. We first identified the labeled neuronal cell bodies in every third non-counterstained section under a light microscope with a 20× or 40× objective lens by means of the optical dissector method (Coggeshall and Lekan 1996), and draw the labeled soma with the camera-lucida. The position of each labeled neuronal cell body was determined on the basis of the position of the cytoarchitectonically delineated thalamic nuclei in the neighboring counterstained sections. We, then,

counted the labeled neuronal cell bodies in each thalamic nucleus.

Results

Anterogradely labeled axon terminals from the OPC

In the first experiment, we examined the features of cortical projections from the OPC. As in our previous study (Sato et al. 2020), the OPC was electrophysiologically identified by recording of responses to electrical stimulation of the contralateral masseter nerve or to passive sustained jaw-openings (e.g. Fig. 2a, b). Then, BDA was electrophoretically injected as an anterograde tracer into the recording sites with the largest responses in seven rats.

These BDA injection sites showed two immunoreactive zones of tracer deposit (an inner, densely labeled zone; and an outer, lightly labeled zone) (e.g. Figs. 2d, e, 4b, c) as
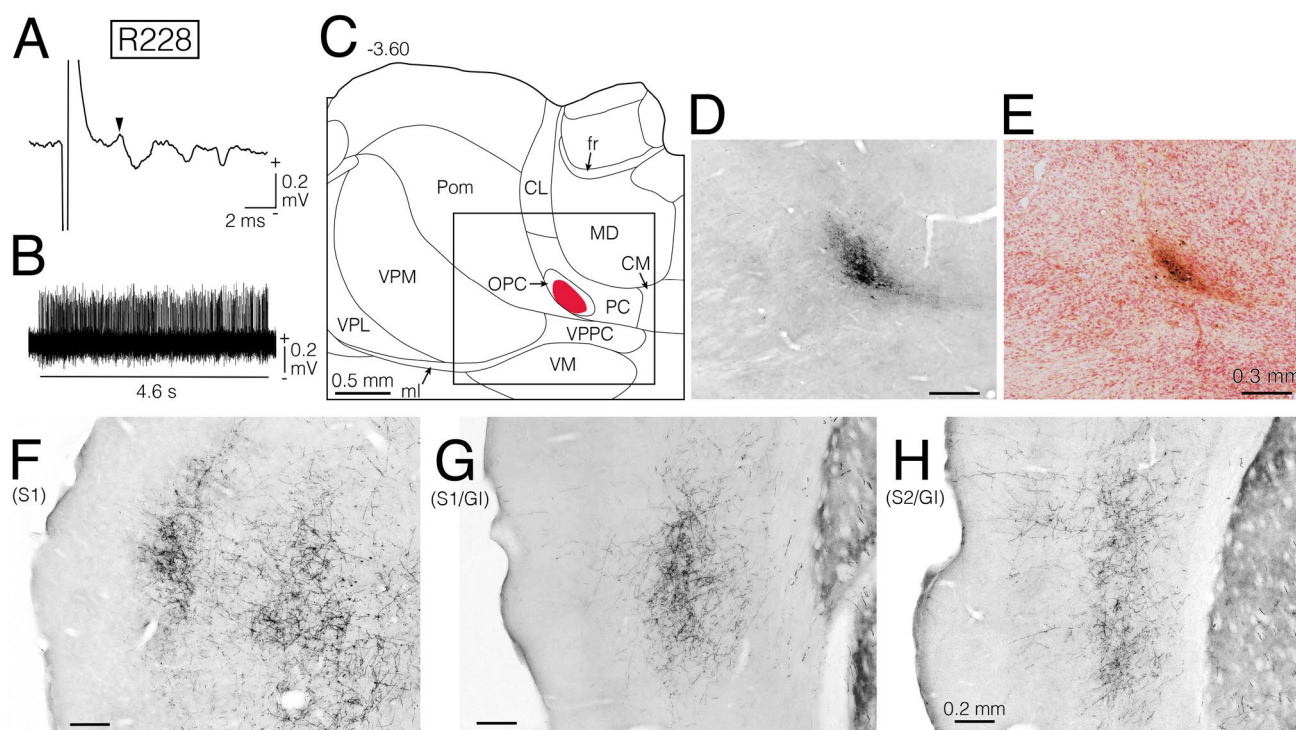

Fig. 2 Field potentials recorded in the OPC (**a**, **b**), an injection site of anterograde tracer, biotinylated dextranamine (BDA), made at the recording site (**c-e**), and the resultant distribution of anterogradely BDA-labeled axonal fibers and terminals in the cerebral cortex (**f–h**) in rat R228. **a**, **b** Extracellular field potentials in response to electrical stimulation of the masseter nerve contralateral to the recording site (an arrowhead indicates a 3.8 ms latency) (**a**), and extracellular multi-unit discharges recorded during a sustained jaw-opening (for about 4.6 s, as indicated by the horizontal bar) (**b**). **c–h** Coronal sections. **c–e** A red area in **c** denotes a BDA injection site. The number in **c** denotes the distance in millimeters caudal (–) to bregma. The boxed area in **c** corresponds to the areas presented in photomicrographs **d** and **e**, both of which show a BDA deposit injected in the OPC. The section **d** is not counterstained, while the section **e** is counterstained with Neutral red. Sections **d** and **e** were collected from the continuous sections. **f–h** Photomicrographs **f–h** showing BDA-labeled axon fibers and terminals located mainly in the rostral region of the primary somatosensory cortex (S1), the rostroventral S1 and rostral GI, and the rostral S2 and rostrocaudally middle GI, respectively. Areas in the photomicrographs **f–h** correspond to the boxed areas in Fig. 3b–d, respectively. Sections **f–h** are not counterstained. For abbreviations, see the abbreviations list

reported in earlier studies (Leak and Moore 2001; Kriegsfeld et al. 2004; Chang et al. 2009; Yoshida et al. 2009). Leak and Moore (2001) and Kriegsfeld et al. (2004) have indicated that the zone of uptake and transport of injected BDA includes the inner and outer BDA-immunoreactive zones by comparing the pattern of retrograde labeling with the pattern predicted by localized injections of BDA. Thus, we followed their estimate to define the extent of effective BDA injection sites (containing the inner and outer immunoreactive zones) found in non-counterstained sections. Then, the extent of effective BDA injection sites was located on the basis of the position observed cytoarchitectonically in the neighboring counterstained sections (e.g. Figs. 2c, 4a); the detailed cytoarchitecture of the OPC has been demonstrated in our previous study (Sato et al. 2020). In all the seven rats, the BDA injection sites covered at least a part of the OPC. In three (R228, R125, and R207) of the seven rats the injection sites were well confined within the OPC (e.g. rat R228, Fig. 2c–e), but in the remaining four rats (R116, R311, R220, and R625), the injected BDA deposit in the OPC extended into the PC adjacent to the OPC.

In the three rats (R228, R125, and R207) with BDA injection sites covering most parts of the OPC (e.g. Fig. 2c–e for rat R228), the anterogradely BDA-labeled axon terminals showed similar distribution patterns. The BDA-labeled axon fibers and terminals were mostly found in the somatosensory cortex (S1 and S2) and the GI only on the side ipsilateral to the BDA injection site (Fig. 3), but not in the motor cortices (Agl and Agm) and the other cortices (medial prefrontal cortex, orbital cortex, or piriform cortex). In the S1, axon fibers and terminals were labeled in the rostroventral one-fourth of the S1 (Figs. 2f, g, 3a–c, j), which mostly corresponds to the intraoral and perioral regions of the S1 demonstrated by Tomita et al. (2012) and Haque et al. (2012). The highest density of BDA-labeled axonal boutons was seen in layer IV of the dorsoventral center of the rostralmost S1 (Fig. 3a–d, f, j). A slightly high density of labeled axonal boutons was also seen in the outer part (Va) and inner part (Vb) of layer V, and the layer VI. The S1 region containing the dense labeling continued ventrally to the dorsal part of the rostral GI (Figs. 2g, 3b, c, j) and caudally to the rostral S2 (Figs. 2h, 3d, j). In the S2, BDA-labeled axonal fibers and terminals were mainly found in the rostral S2 (Figs. 2h, 3d, j), which largely corresponds to the intraoral and perioral regions of the S2 revealed by Haque et al. (2012). A slightly high density of labeled axonal boutons was seen in layers IV–VI of the rostral S2 including the rostralmost S2 (Figs. 2h, 3d, h); the rostralmost S2 is known to slightly receive the JCMS proprioceptive inputs via the VPMcvm (Sato et al. 2017). It is noteworthy that the density of labeled axonal boutons in layer IV was not so high, when compared with layer IV of the S1 described above (compare Fig. 3h with Fig. 3f). The S2 region containing the dense labeling continued rostrally

to the rostroventral part of the S1, and ventrally to the dorsal part of the caudal GI (Figs. 2h, 3d, j). We cytoarchitectonically divided the insular cortex into three dorsoventral parts: the GI, the DI, and the agranular insular cortex (AI) as in earlier studies (Cechetto and Saper 1987; Allen et al. 1991; Paxinos and Watson 1998; Sato et al. 2013, 2017) (e.g. Figs. 1, 3, 5, 6). The BDA-labeled axonal fibers and terminals in the insular cortex were mostly restricted to the GI, which largely corresponds to the orofacial region of the GI demonstrated by Sato et al. (2013) (Figs. 2g, h, 3). Additionally, the labeling was slightly seen in the adjacent DI, but not in the AI. A high density of axonal boutons was labeled in layers Vb and VI in the dorsal part of the rostrocaudally middle GI, which included the dGIrvs2 (its center is at about 0.9 mm rostral to bregma) (Figs. 2g, h, 3c, d, g); the dGIrvs2 receives strong JCMS proprioceptive inputs via the VPMcvm (Sato et al. 2017). It is notable that the density of labeled boutons in layer IV was very low.

In the remaining four rats (R116, R311, R220, and R625) with the BDA injection sites extending to the PC, the BDA-labeled terminals showed the combination of terminal distribution patterns in the above three rats (R228, R125, and R207) and those in the rats where the BDA injection was confined to the PC (as described below).

Anterogradely labeled axon terminals from the caudal PC

In the second experiment, we sought to examine the distribution pattern of axonal fibers and terminals arising from the caudal PC, which is adjacent to the OPC. After identifying the OPC as in the first experiment, we shifted the electrode 0.2–0.3 mm dorsally and 0.4–0.6 mm rostrally from the OPC, and made a small BDA injection in six rats. In all the six rats, the BDA injection sites were histologically confirmed to cover at least a part of the PC. In three (R213, R206, and R225) of the six rats, the BDA injection sites were confined to the caudal PC rostrally adjacent to the OPC, and did not cover the OPC (e.g. in rat R213, Fig. 4a–c). In these three rats, the BDA-labeled axonal fibers and terminals showed similar distribution patterns in the cortex on the side ipsilateral to the injection site. The labeled axons were mostly found in the lateral part of the rostralmost Agm and the rostral Agl (Figs. 4d, 5). In the lateral part of the rostralmost Agm, a slightly high density of labeled axonal boutons was seen in layers VI and V (Figs. 4d, 5a, f), whereas in layers V and II/III of the rostral Agl (Fig. 5b, c, g). In addition, the BDA labeling was seen in the dorsolateral orbital cortex and the rostralmost and caudalmost parts of the DI and AI in the insular cortex (Figs. 4d, 5). A low density of boutons was mainly labeled in layers VI and Vb of the DI and in layers V and VI of the AI (Fig. 5b, c, h, i); we should note that layer V of the AI could not be cytoarchitectonically divided
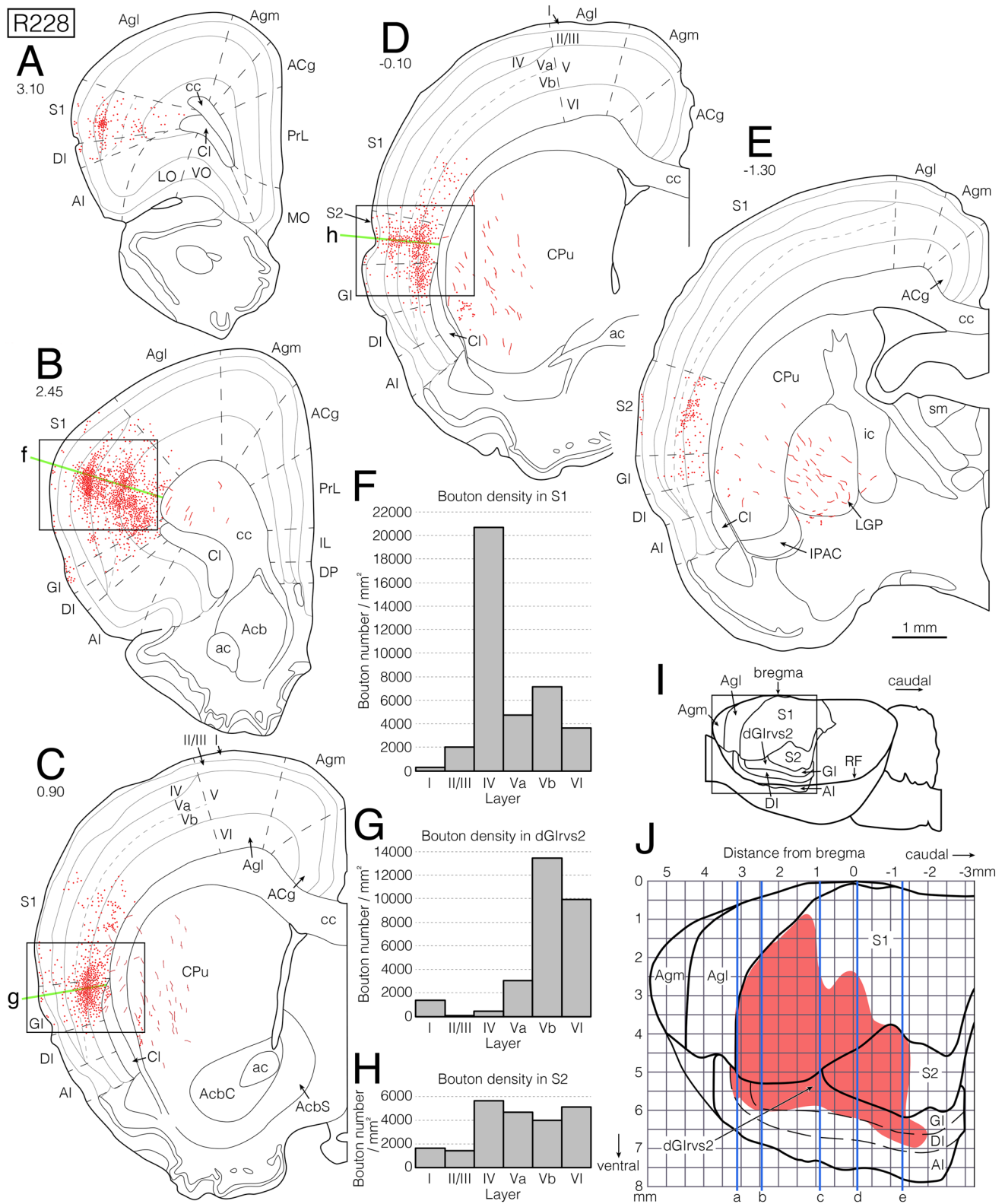
into its inner and outer parts. Importantly, no axon labeling was observed in the somatosensory cortex (S1 and S2), the GI, the medial prefrontal cortex (such as the anterior cingulate cortex, the prelimbic cortex, and infralimbic cortex),

and the piriform cortex. These results indicate that although the OPC and caudal PC are contiguous in the thalamus, the cortical projection sites from the OPC were clearly distinct from those from the caudal PC (compare Fig. 3 with Fig. 5).

◀**Fig. 3** Semi-schematic drawings showing the distribution of antero-gradely BDA-labeled axons (red short lines and dots) (**a–e**), the distribution of density of labeled axonal boutons per individual cortical layers (**f–h**), and a lateral view of the distribution of labeled axons in the cerebral cortex (**i**, **j**), after a BDA injection into the OPC in rat R228. The injection site is presented in Fig. 2c–e. **a–e** Drawings of coronal sections are arranged rostrocaudally from **a** to **e**. Numbers denote the distance in millimeters rostral or caudal (–) to bregma. The rostrocaudal levels of sections **a–e** are also indicated by blue vertical lines **a–e**, respectively, in **j**. Note that the labeled axons in the cortex were found only on the side ipsilateral to the injection site. The boxed areas in **b–d** correspond to areas shown in Fig. 2f–h, respectively. **f–h** The distribution of density (number/mm^2) of labeled axonal boutons found in each cortical layer at the positions indicated by green lines **f** (in **b**), **g** (in **c**), and **h** (in **d**), respectively. We should note that the individual green line indicates the center of the long strip-shaped area for counting the labeled boutons (the same is applied to Fig. 5). **i** A lateral view of the left brain showing the location of the cortical areas. The boxed area corresponds to the area shown in **j**. **j** A lateral view of the distribution (red area) of labeled axons in the cortex. The numbers along the abscissa denote the distance rostral or caudal (–) to bregma, and those along the ordinate denote the distance ventral to bregma. For abbreviations, see the abbreviations list

In the remaining three (R227, R350, and R106) of the six rats with the injected BDA deposits in the caudal PC extending into the OPC, the BDA-labeled terminals showed the combination of terminal distribution patterns in the above three rats (R213, R206, and R225) and those in the rats where the BDA injection was confined to the OPC.

Retrogradely labeled intralaminar and sensory thalamic neurons from the S1, S2, and GI

In the third experiment, we sought to confirm that the OPC contained projection neurons to multiple cortical areas, and compare the robustness of cortical projections from the OPC with that from the other intralaminar thalamic nuclei (CL, PC, CM, and PF) and from so-called sensory thalamic nuclei (core VPM, VPMcvm, VPPC, Pom, and Sm). In a total of 23 rats, we injected a retrograde tracer FG in the multiple cortical areas where we found many anterogradely BDA-labeled axon terminals from the OPC in the first experiment. The FG injection sites showed three immunoreactive zones of tracer deposit (an inner, necrotic center; a middle, densely labeled zone; and an outer, lightly labeled zone) as reported in earlier studies (Moga and Saper 1994; Leak and Moore 2001; Kriegsfeld et al. 2004; Chang et al. 2009; Yoshida et al. 2009). Again, Leak and Moore (2001) and Kriegsfeld et al. (2004) have estimated that the zone of uptake and transport of injected FG includes all the three FG-immunoreactive zones by comparing the pattern of retrograde FG labeling with that predicted by localized injection of anterograde tracer. According to their estimate, we first defined the extent of effective FG injection sites in non-counterstained sections. We, then, exactly located the extent of effective

FG injection sites by reference to the position observed cytoarchitectonically in the neighboring counterstained sections (e.g. Figs. 6b, 7a, d for rat R902; Figs. 6b, 7f, i for rat R313; Figs. 6b, 8a, d for rat R038).

In 12 out of the 23 rats, the FG injection was restricted to any of the following five regions (Fig. 6; Table 1): (1) the rostral S1, which corresponds to the intraoral or perioral region of the S1 (Haque et al. 2012; Tomita et al. 2012), (2) the rostralmost S2 including the S2 region where the VPM-cvm receiving JCMS proprioceptive inputs weakly projects (Sato et al. 2017), (3) the rostral S2 excluding the rostralmost S2 (It is noteworthy that the rostral S2 corresponds to the intraoral or perioral region of the S2 [Haque et al. 2012]), (4) the rostrocaudally middle level of the GI including the dGIrvs2, where the VPMcvm receiving JCMS proprioceptive inputs strongly projects (Sato et al. 2017), and (5) the GI caudal to the dGIrvs2 [the dGIrvs2 and the GI caudal to the dGIrvs2 correspond to the perioral region of the GI (Sato et al. 2013)]. As shown in Table 1, we counted FG-labeled neurons in the OPC, in the other intralaminar thalamic nuclei (CL, PC, CM, and PF), and in the sensory thalamic nuclei (core VPM, VPMcvm, VPPC, Pom, and Sm) after FG injections into the five cortical regions. We excluded the remaining 11 rats from the subsequent analysis since the FG injection sites covered two of the five identified cortical regions, or extended outside the cortical areas.

In three rats (R902, R305, and R403), FG injection was confined to the rostral S1. In rat R902, FG deposit mainly covered layers IV-VI (Fig. 7a, d) and rostrally extended into layers II and III. In rat R305, FG deposit mainly covered layers I–Vb, whereas all layers II–VI in rat R403. These results indicated that all the three injections mostly covered layers IV-VI of the rostral S1, where the OPC projected in the first experiment. In all the three rats, retrogradely FG-labeled neurons showed similar distribution patterns in the intralaminar thalamic nuclei and the sensory thalamic nuclei (Fig. 7b, c, e). The high percentage (25.2%) of neurons was labeled in the OPC (Fig. 7b, e; Table 1); this percentage was much higher than the percentage in the other intralaminar nuclei and the sensory thalamic nuclei except for the core VPM (53.7%).

In two rats (R313 and R829), FG was injected into the rostralmost S2. The FG injection sites mainly covered layers Va-VI in both rats (e.g. Fig. 7f, i), but also covered layer IV only in rat R829. Thus, both injection sites covered cortical layers of the rostralmost S2 where the OPC projected in the first experiment. In both rats, retrogradely FG-labeled neurons showed similar distribution patterns in the intralaminar thalamic nuclei and the sensory thalamic nuclei (Fig. 7g, h, j). The high percentage (29.1%) of labeled neurons was found in the OPC (Fig. 7g, j; Table 1); this percentage was comparable to the percentage in the core VPM (29.6%) and the VPMcvm (23.5%).
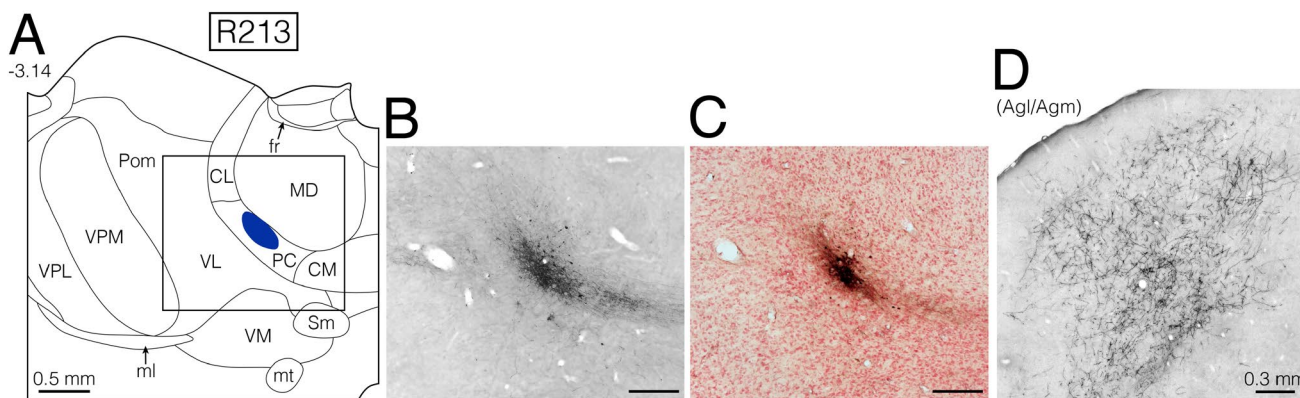
Fig. 4 An injection site of anterograde tracer BDA made in the caudal part of the PC (**a**–**c**), and the resultant anterogradely BDA-labeled axonal fibers and terminals (**d**) in rat R213. **a**–**d** Coronal sections. **a**–**c** Number in **a** denotes the distance in millimeters caudal (−) to bregma. The boxed area in **a** corresponds to the areas shown in photomicrographs **b** and **c**, both of which show a BDA deposit injected in the PC. The section **b** is not counterstained, whereas the section **c** is counterstained with Neutral red. Sections **b** and **c** were collected from the continuous sections. **d** A photomicrograph showing BDA-labeled axonal fibers and terminals in the lateral region of the rostral-most level of the medial agranular cortex and the rostralmost level of the lateral agranular cortex, which corresponds to the boxed area in Fig. 5a. Section **d** is not counterstained. For abbreviations, see the abbreviations list

In two rats (R818 and R819), FG was injected into the rostral S2 excluding the rostralmost S2. The FG deposit mainly covered layers I–Vb in rat R818, and layers II–VI in rat R819, indicating that both injection sites covered the overall cortical layers of the rostral S2 excluding the rostralmost S2. In both rats, retrogradely FG-labeled neurons showed similar distribution patterns in the intralaminar thalamic nuclei and the sensory thalamic nuclei. The percentage (10.8%) of labeled neurons in the OPC was higher than the percentage in the other intralaminar nuclei and the sensory thalamic nuclei except for the core VPM (71.8%) and the Pom (11.9%), but was not so high in comparison to the other injection cases (Table 1).

In three rats (R038, R216, and R113), FG injection was made into the rostrocaudally middle level of the GI including the dGIrvs2, where the VPMcvm receiving JCMS proprioceptive inputs strongly projects (Sato et al. 2017). In rat R038, FG injection site mainly covered layers II–VI (Fig. 8a, d). In rats R216 and R113, FG injections mainly covered layers Va–VI. These results indicated that the three injection sites mostly covered the cortical layers of the rostrocaudally middle level of the GI including the dGIrvs2 where the OPC projected in the first experiment. In all the three rats, FG-labeled neurons demonstrated similar distribution patterns in the intralaminar thalamic nuclei and the sensory thalamic nuclei (Fig. 8b, c, e). A relatively high percentage (17.7%) of labeled neurons was seen in the OPC (Fig. 8b, e), but this percentage was higher than the percentage in the other intralaminar nuclei and the sensory thalamic nuclei except for the VPPC (42.1%) and the VPMcvm (35.7%) (Table 1).

In two rats (R830 and R208), FG was injected into the GI caudal to the dGIrvs2. In rat R830, FG deposit mainly covered layers II–VI, whereas layers IV–VI in rat R208. Both injection sites well covered the cortical layers of the GI caudal to the dGIrvs2, where the OPC projected in the first experiment. In both rats, retrogradely FG-labeled neurons showed similar distribution patterns in the intralaminar thalamic nuclei and the sensory thalamic nuclei. The high percentage (25.2%) of labeled neurons was seen in the OPC (Table 1); this percentage was much higher than the percentage in the other intralaminar nuclei and the sensory thalamic nuclei except for the VPPC (48.0%).

In summary, we concluded that, among the intralaminar and sensory thalamic nuclei, the OPC was only the structure that projected to all of the five cortical areas tested in the present study.

Discussion

As summarized in Fig. 9, the present study has identified a new corticopetal pathway conveying JCMS proprioception, which is one of orofacial sensations. A combination of anterograde tracer injections into the OPC and retrograde tracer injections into the cerebral cortex has revealed that the OPC strongly projects ipsilaterally to the rostral regions of the S1 and S2, and to almost all of the rostrocaudal levels of the GI (thick red routes in Fig. 9). This finding suggests that the corticopetal pathway from the OPC has broad projection features, in comparison to the other corticopetal pathways that convey orofacial sensations, such as cutaneous/mucosal sensations, relayed via the core VPM or the Pom mainly to the S1 and S2 (pale-green routes in Fig. 9), nociception or thermal sensation relayed via the Sm to the orbital cortex

(pale-purple route), taste sensation relayed via the VPPC principally to the DI (pale-gray route), and JCMS proprioceptive sensation relayed via the VPMcvm mostly to the dGIrvs2 (thin red route).

Comparison of thalamocortical routes related to the other sensory inputs

Proprioceptive inputs arising from orofacial muscles, as well as from other body muscles, can be recorded in the somatosensory cortex, mainly in area 3a of the S1 in humans (Gandevia and Macefield 1989; Macefield et al. 1989), monkeys (Phillips et al. 1971; Iwamura et al. 1983; Sirisko and Sessle 1983), and cats (Amassian and Berlin 1958; Oscarsson and Rosen 1963, 1966; Landgren and Silfvenius 1969; Phillips et al. 1971; Lund and Sessle 1974; Iwata et al. 1985; Gandevia and Macefield 1989; Macefield et al. 1989). On the other hand, the area 3b of the S1 mainly receives cutaneous sensation in monkeys and cats (Powell and Mountcastle 1959; Heath et al. 1976; Felleman et al. 1983; Iwamura et al. 1983). However, it remained unclear in rats whether the muscle proprioceptive and cutaneous inputs might be segregated or integrated within the S1.

One of the most important findings in this study was that the OPC conveying the JCMS proprioceptive sensation strongly projected to all of the S1, S2, and GI, whereas the core VPM and Pom, both of which could carry the orofacial cutaneous sensation or deep sensation excluding the JCMS proprioceptive sensation, strongly projected to the S1 and S2, but very slightly to the GI.

With respect to projections to the rat S1, the OPC efferents terminated mainly in layer IV and considerably in layers Va, Vb, and VI in the present study. In contrast, the core VPM is known to project mainly to layer IV and outer part of layer VI (also the inner part of layer III or the layer Vb) (Herkenham 1980; Zhang and Deschêses 1998; Pierret et al. 2000; Furuta et al. 2011), whereas the Pom mainly projects to layers I and Va (Herkenham 1980; Zhang and Deschênes 1998; Pierret et al. 2000; Ohno et al. 2012). Therefore, cortical projection patterns from the OPC to the S1 closely resembled those from the core VPM (but not the Pom) in terms of projections to cortical layers. Importantly, however, Sato et al. (2017) have also demonstrated that the thalamic lingual area, which is located in the caudomedial part of the core VPM and conveys the lingual cutaneous sensation, sends projections to layer IV of the rostroventral region of the S1 (see Fig. 9 of Sato et al. 2017). The S1 subregion receiving the thalamic lingual area appears to be located more caudoventrally than layer IV of the S1 subregion receiving inputs from the OPC demonstrated in the present study, although both subregions overlap to some extent. Taken together, it is likely that the convergence of the OPC–S1 and core VPM–S1 pathways in layer IV is limited,

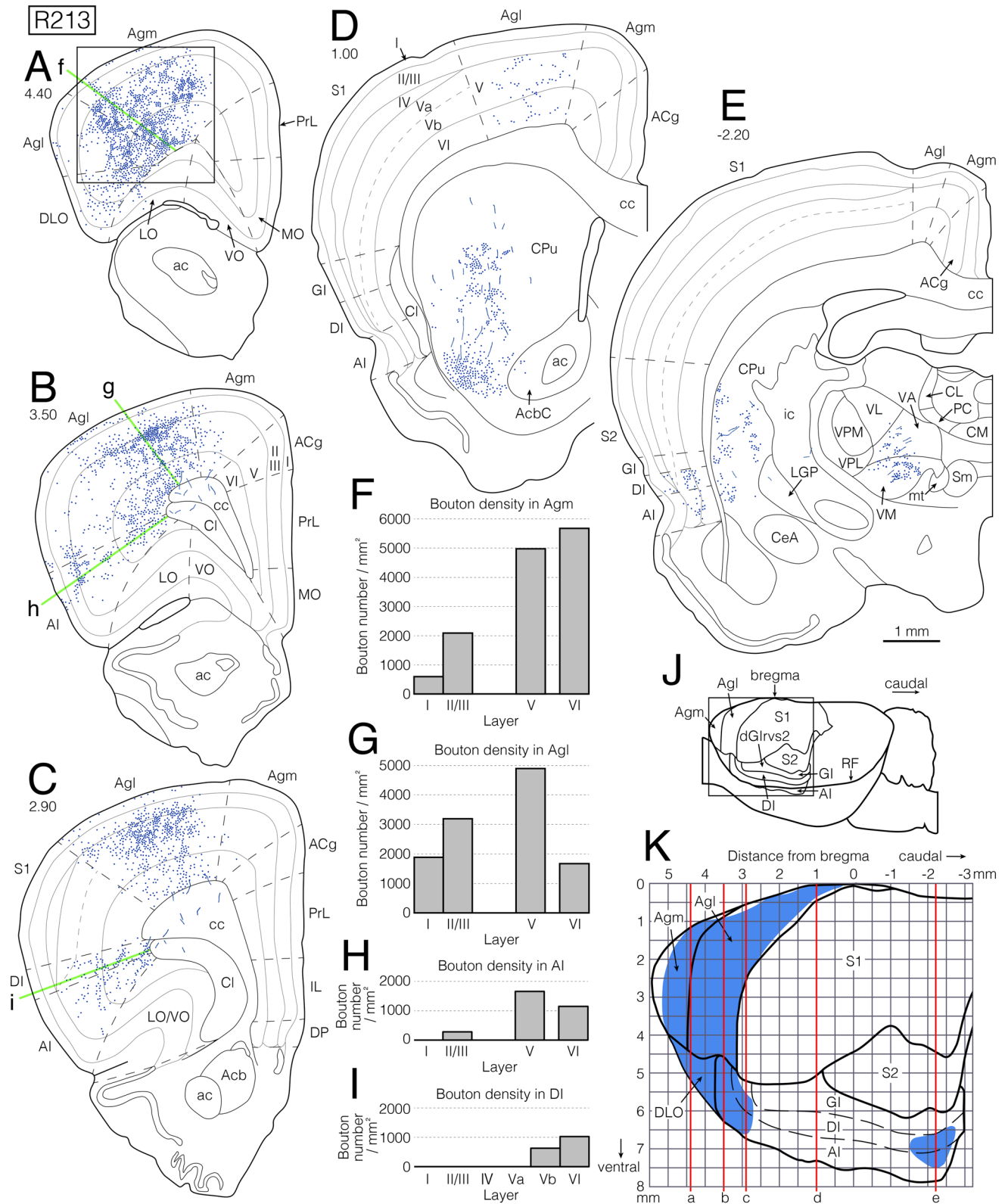but rather that the proprioceptive sensation and the cutaneous sensation are separately processed in the rat S1.

With regard to projections to the rat S2, the OPC projected evenly to layers IV, Va, Vb, and VI. The core VPM projects to layers IV and VI of the S2 (Pierret et al. 2000), whereas the Pom projects to layers Va and I of the S2 (Zhang and Deschênes 1998; Ohno et al. 2012). These data suggest that sensory integration of proprioceptive and cutaneous sensations might occur in layers IV, Va, and VI of the S2 in comparison to the S1.

With respect to projections to the rat GI, the OPC principally projected to layers Vb and VI, but the core VPM and Pom did not send projections to the GI. The proprioceptive information carried by the OPC–GI pathway may independently influence subcortical motor structures, such as the thalamus, lower brainstem, and spinal cord, through the output neurons in layers Vb and VI.

Comparison of thalamocortical routes related to JCMS proprioceptive inputs

The proprioceptive sensation from the body has been considered to be conveyed to the rostrodorsal shell or rostral (oral) region (VPLo) of the VPL (monkey, Friedman and Jones 1981; Maendly et al. 1981; Jones and Friedman 1982; Jones et al. 1982; cat: Andersson et al. 1966), and, thus, the relay site for orofacial proprioceptive sensation has been predicted to be located in the rostrodorsal shell of the VPM medially adjacent to the VPLo (Jones and Friedman 1982). However, a series of our studies (Yoshida et al. 2017; Sato et al. 2020) has revealed that the efferent axons from the Su5 receiving JCMS proprioceptive inputs terminate in the OPC as well as in the VPMcvm (but not in the rostrodorsal shell of the VPM). The OPC was initially isolated from the PC in the rodent thalamus as an ovoid region on the basis of its cytoarchitectonic features (Paxinos and Watson 1986; Jones 2007), but it has not been found in other animal species including primates. The reason why we succeeded to find the OPC and VPMcvm as the thalamic nuclei receiving the orofacial proprioception is that we performed a combination of electrophysiological and neuronal tracing techniques to reveal the thalamic projections from the rat Su5, which receives strong JCMS proprioceptive inputs (Fujio et al. 2016; Yoshida et al. 2017; Sato et al. 2020). Thus, we can presume that, in animal species other than rats, there exist the Su5–OPC/VPMcvm pathways or the Su5–alternative thalamic subgerions pathways, which convey the JCMS proprioception.

Our previous study (Sato et al. 2017) has demonstrated the JCMS proprioceptive sensation is conveyed via the VPMcvm to a very restricted cortical area of the rostrocaudally middle level of the GI (dGIrvs2). The present retrograde tracing confirmed the OPC-insula pathway as well as the VPMcvm-insula

pathway. Thus, we have concluded that there exist two thalamo-insular pathways that convey JCMS proprioceptive sensations from the OPC and VPMcvm. Notably, the dGIrvs2

seems to be only the structure that receives proprioceptive inputs from both the OPC and VPMcvm. However, the OPC sent axon terminals mostly in layers Vb and VI of the dGIrvs2,

whereas the VPMcvm gives off terminals mostly in layer IV of the dGIrvs2 (Sato et al. 2017). These results indicate that the proprioceptive inputs from the OPC and VPMcvm may not necessarily be integrated in the dGIrvs2, but rather distinctively processed. In the relationship between proprioceptive sensation and motor commands, repetitive electrical stimulation of rat insular cortex induces rhythmical jaw movements (Zhang and Sasamoto 1990; Satoh et al. 2007; Maeda et al.

2014); the effective sites are so large that they seem to partly cover the dGIrvs2. The proprioceptive inputs from the OPC in layers Vb and VI of the dGIrvs2 may directly influence the subcortical motor structures, such as the brainstem, spinal cord, and thalamus. Indeed, the direct pathway from the dGIrvs2 to the Su5, which includes premotor neurons projecting to the jaw-closing and -opening motoneurons, has morphologically been demonstrated (Ikenoue et al. 2018).

The GI is historically considered to be involved in the integration of multimodal sensations, such as somatic sensation including nociception, visceral sensation, gustation, olfaction, and hearing in humans (Augustine 1985, 1996), monkeys (Mesulam and Mufson 1982) and rats (Yamamoto et al. 1981, 1988, 1989; Ito 1992; Hanamori et al. 1998a, b; Ogawa and Wang 2002; Gauriau and Bernard 2004). In fact, the present study has revealed the strong projection to the GI from the VPPC (so-called gustatory thalamus), which is well known to relay gustatory and visceral information (Benjamin and Pfaffmann 1955; Benjamin and Akert 1959; Cechetto and Saper 1987; Nakashima et al. 2000). Again,
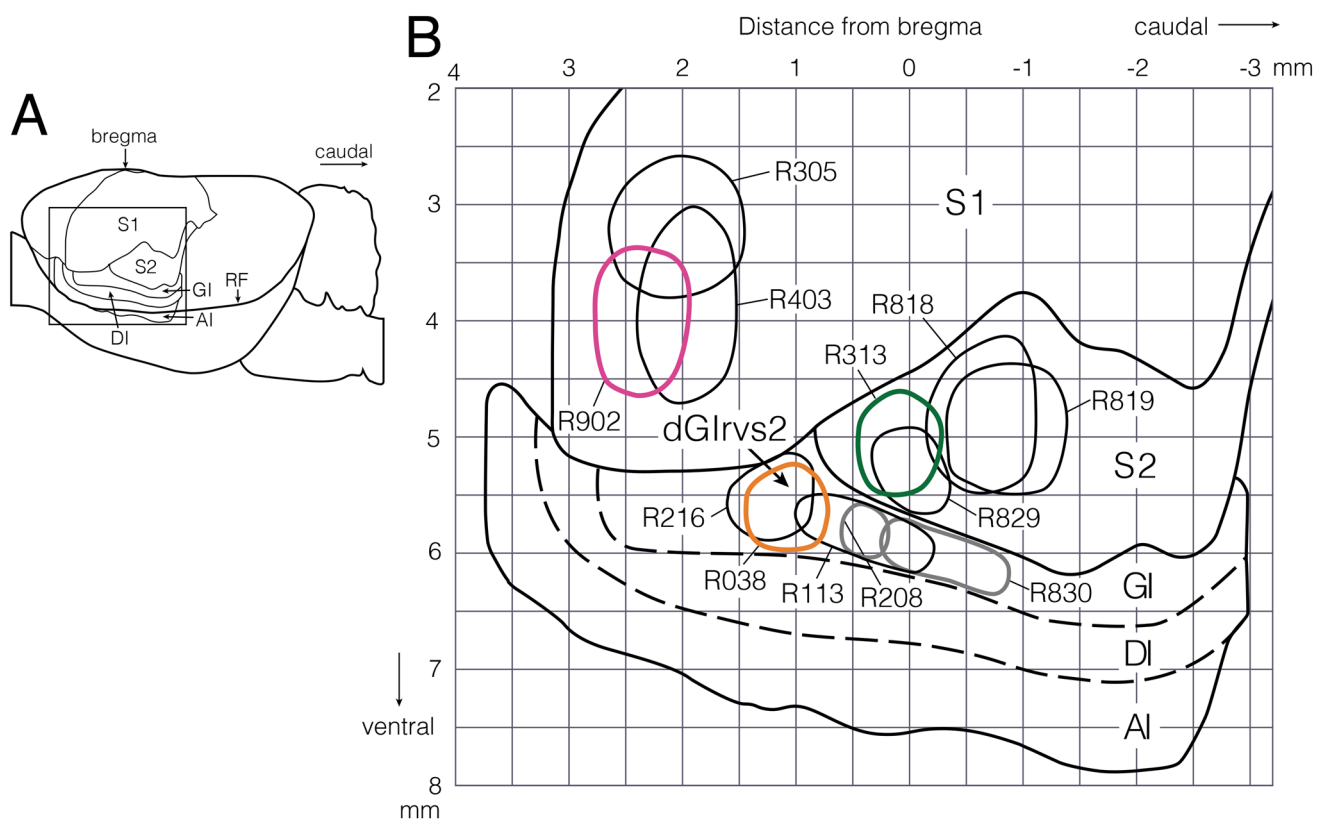

Fig. 6 Lateral views of the left brain (**a**) and injection sites of a retrograde tracer Fluorogold (FG) made in the rostral S1, the rostralmost S2, the rostral S2 excluding the rostralmost S2, the rostrocaudally middle level of the GI including the dGIrvs2, and the GI caudal to the dGIrvs2 (**b**). **a** The boxed area corresponds to the area shown in **b**. **b** Each FG injection site is surrounded by a solid line and is labeled with the rat number. The pink, green and orange lines show injection sites in rats R902, R313, and R038, where experimental results are presented in Figs. 7a–e, 7f–j, and 8a–e, respectively. Note that the injection sites in rats R313 and R829 covered the rostralmost S2. The injection sites in rats R216, R038, and R113 partly covered the dGIrvs2, whereas those in rats R208 and R830 did not. For more information, see the Fig. 3j legend
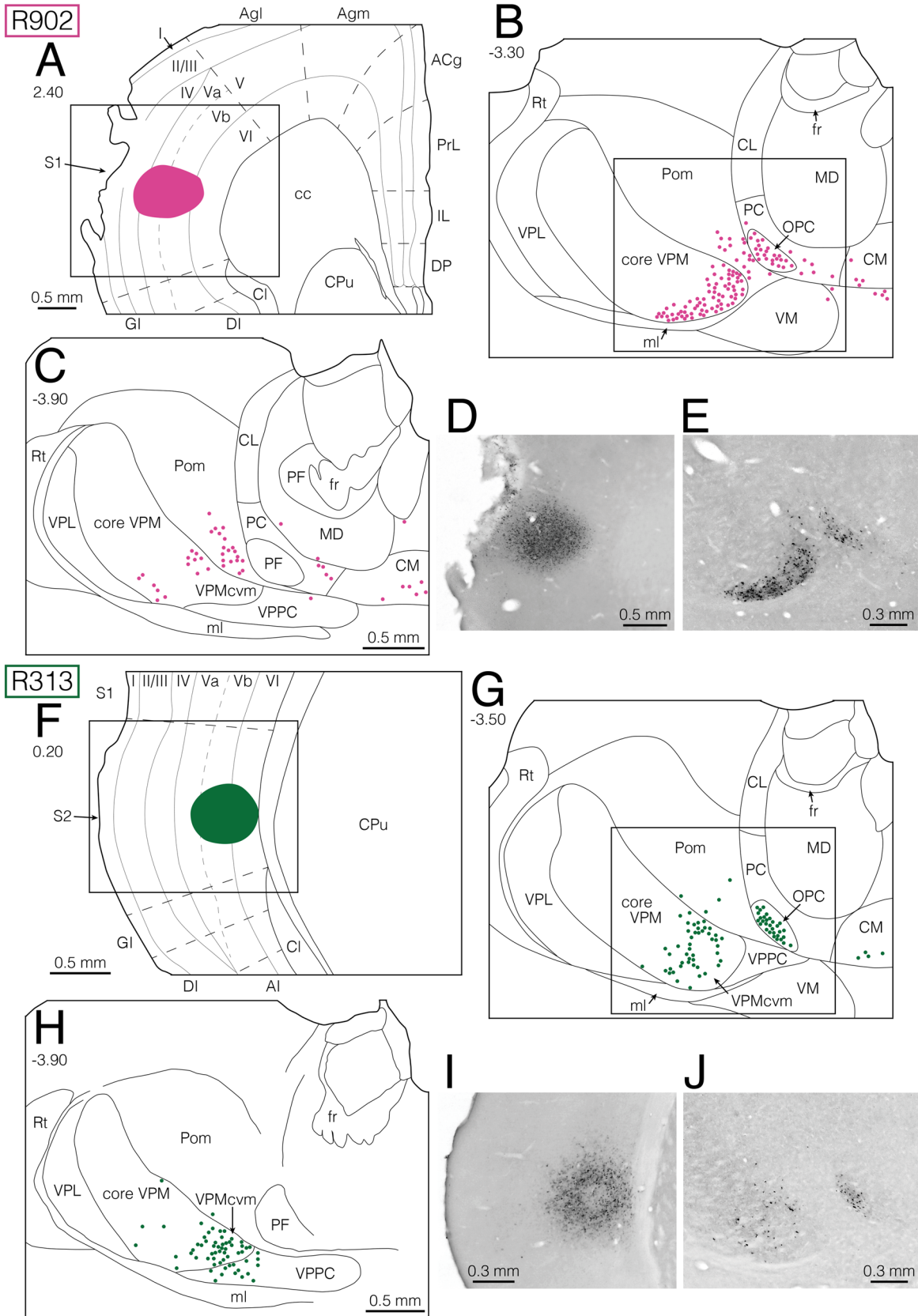
◀**Fig. 7** Semi-schematic drawings showing FG injection sites in the rostral S1 (**a**) and the rostralmost S2 (**f**), and the resultant retrogradely FG-labeled neurons found at the level of the OPC (**b**, **g**) and at the level slightly caudal to the OPC (**c**, **h**), and photomicrographs showing FG injection sites shown in **a** and **f** (**d**, **i**) and the resultant retrogradely FG-labeled neurons shown in **b** and **g** (**e**, **j**). Sections **a–e** and **f–j** are obtained from rat R902 and rat R313, respectively. **a–j** Coronal sections. The numbers in **a–c** and **f–h** denote the distance in millimeters rostral or caudal (–) to bregma. **a**, **f** FG injection sites are denoted by a pink area (**a**) and a green area (**f**), respectively. A lateral view containing both injection sites is shown in Fig. 6b. The boxed areas in **a** and **f** correspond to the areas shown in photomicrographs **d** and **i**, respectively. **b**, **c**, **g**, **h** Retrogradely labeled neuronal cell bodies are denoted by pink dots in rat R902, and green dots in rat R313. The boxed areas in **b** and **g** correspond to the areas shown in photomicrographs **e** and **j**, respectively. Sections **d**, **e**, **i** and **j** are not counterstained. For abbreviations, see the abbreviations list

however, the VPPC principally projects to layer Va in the rat GI (Nakashima et al. 2000); this layer is different from the layers (layers Vb and VI, and layer IV) where the OPC and VPMcvm mainly projected. Therefore, it remains still unclear whether the GI might be the site for the integration of JCMS proprioceptive sensations from the OPC/VPMcvm and the other orofacial sensations.

Significance of the OPC within the intralaminar thalamic nuclei

The intralaminar thalamic nuclei are known to be involved in motor functions by receiving projections from motor-related structures, such as the substantia nigra and cerebellum, and by projecting to the striatum and cerebral motor cortices

Fig. 8 Semi-schematic drawings showing an FG injection site (orange area) in the rostro-caudally middle level of the GI including the dGIrvs2 (**a**) and the resultant retrogradely FG-labeled neurons (orange dots) found at the level of the OPC (**b**) and at the level slightly caudal to the OPC (**c**), and photomicrographs showing an FG injection site presented in **a** (**d**) and the resultant retrogradely FG-labeled neurons presented in **b** (**e**), in rat R038. The lateral view of injection site is presented in Fig. 6b. The boxed areas in **a** and **b** correspond to the areas shown in **d** and **e**, respectively. For abbreviations, see the abbreviations list. For more information, see the Fig. 7 legend
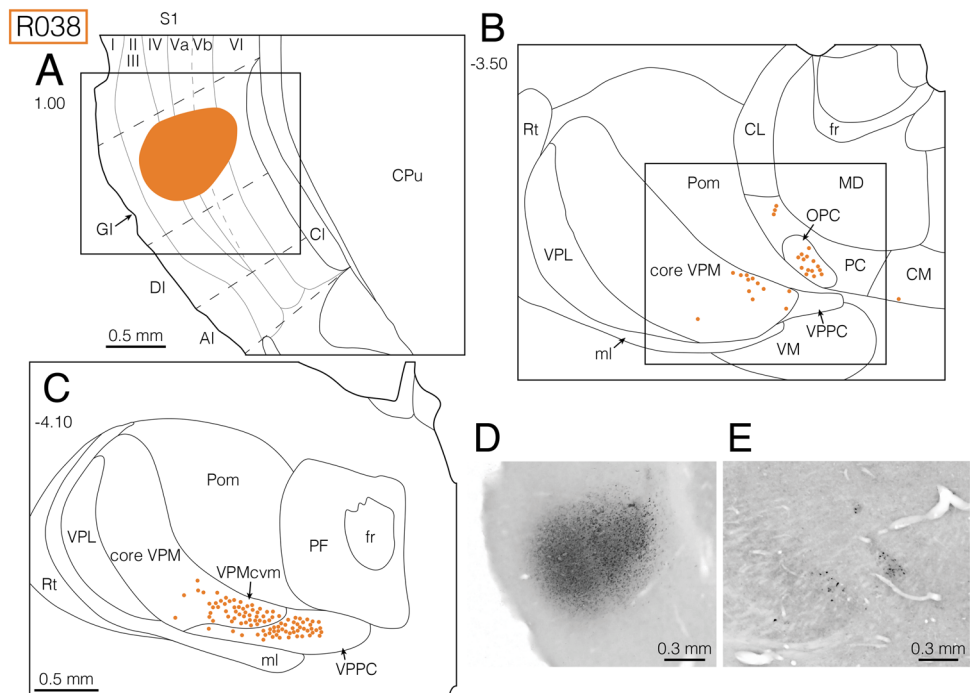

Table 1 Percentages (numbers) of neurons labeled after retrograde tracer injections into the cortex

Injection site rat no	Intralaminar thalamic nuclei					Sensory thalamic nuclei					Total
	OPC	CL	PC	CM	PF	core VPM	VPMcvm	VPPC	Pom	Sm	
Rostral S1 R902	25.2 (113)	0.7 (3)	1.8 (8)	1.6 (7)	0 (0)	53.7 (241)	0.9 (4)	1.3 (6)	14.9 (67)	0 (0)	100 (449)
Rostralmost S2 R313	29.1 (72)	0 (0)	2.8 (7)	3.6 (9)	0 (0)	29.6 (73)	23.5 (58)	8.9 (22)	2.4 (6)	0 (0)	100 (247)
Rostral S2 excluding rostralmost S2 R819	10.8 (105)	0 (0)	1.7 (17)	0 (0)	0.6 (6)	71.8 (700)	0.7 (7)	2.5 (24)	11.9 (116)	0 (0)	100 (975)
dGIrvs2 R038	17.7 (55)	0 (0)	2.3 (7)	2.3 (7)	0 (0)	0 (0)	35.7 (111)	42.1 (131)	0 (0)	0 (0)	100 (311)
GI caudal to dGIrvs2 R830	25.2 (115)	0 (0)	2.0 (9)	15.8 (72)	1.5 (7)	3.3 (15)	0.2 (1)	48.0 (219)	3.9 (18)	0 (0)	100 (456)

Fig. 9 Summary diagram showing all of the corticopetal pathways ▶ that convey orofacial sensations. Thalamocortical pathways from the OPC and the caudal PC (indicated by thick red route and blue route, respectively) revealed in the present study are added to the summary diagram shown in Fig. 1. For abbreviations, see the abbreviations list. For more information, see the Fig. 1 legend and the main text

(Agl and Agm) (Haroian et al. 1981; Berendse and Groenewegen 1991; Groenewegen et al. 1999; Jones 2007; Iwai et al. 2015). Therefore, it is plausible that the intralaminar thalamic nuclei receive orofacial proprioceptive inputs from the JCMS, which can accelerate jaw movements via reflex arches located in the lower brainstem (Dubner et al. 1978; Waite and Tracey 1985; Waite 2004). In this respect, it is of great interest that among the rat intralaminar nuclei, the OPC is the only structure to receive JCMS proprioception (Sato et al. 2020). This earlier finding appeared to indicate that the OPC has quite unique corticopetal projection features that are distinct from those of the other intralaminar nuclei. In fact, the present and earlier studies (Berendse and Groenewegen 1991; Van der Werf et al. 2002) have revealed that only the OPC, among the intralaminar thalamic nuclei, sends strong, wide projections to the S1, S2, and GI, but not to the other cortical areas including the motor cortices (Agl and Agm).

Interestingly, the rostral and rostroventral S1, rostral S2, and almost all of the rostrocaudal levels of the GI (excluding the caudalmost GI), to which the OPC projected, appear to correspond to orofacial regions of the S1, S2, and GI, respectively (Welker and Sinha 1972; Carvell and Simons 1986; Benison et al. 2007; Haque et al. 2012; Tomita et al. 2012; Sato et al. 2013). Among the intralaminar thalamic nuclei, only the OPC receives orofacial proprioceptive inputs via the Su5 (Sato et al. 2020), whereas no intralaminar thalamic nuclei receive ascending projections from the external cuneate nucleus, which receives proprioceptive inputs from neck and forelimb muscles (Uemura et al. 2020). These findings indicate that orofacial proprioception may have unique, important features in the central processing of proprioception arising from the entire body.

So far, the OPC has been found only in the rodent thalamus, as described above. In contrast, the centromedian nucleus is well developed in the anthropoid and human thalamus but not in rodents (Jones 2007). Importantly, both nuclei are located in the internal medullary lamia of the thalamus medial to the VPM. Does the OPC in rodents correspond to the centromedian nucleus in primates? The centromedian nucleus in monkeys sends projections mainly to the motor cortex, premotor cortex, and supplementary motor cortex (Sadikot et al. 1992; Fang et al. 2006; Stepniewska et al. 2007). In contrast, the present data indicate that the rat OPC does not project to the Agl, which corresponds to the primate primary motor cortex (Donoghue and Wise
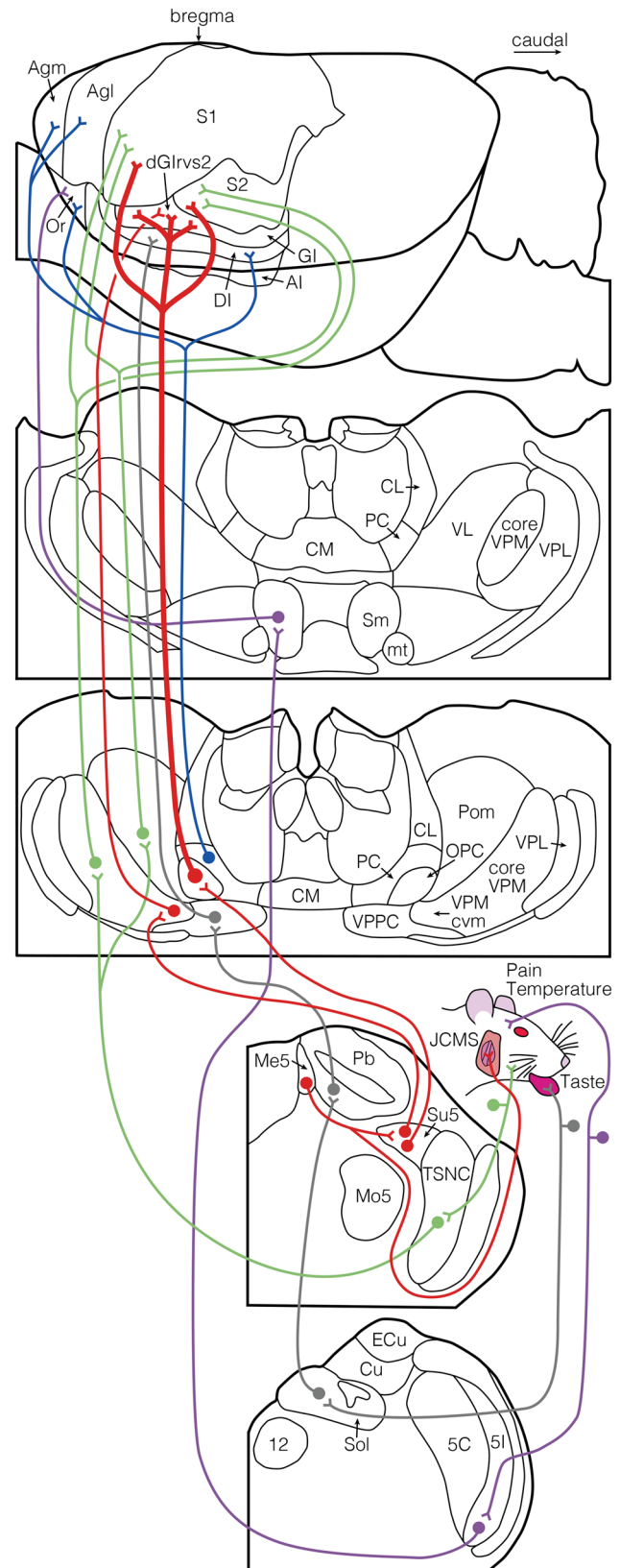
1982; Donoghue and Parham 1983; Yoshida et al. 2009; Haque et al. 2010), and to the Agm, which corresponds to the primate premotor and supplementary motor cortices (Donoghue and Parham 1983; Hicks and Huerta 1991; Van Eden et al. 1992); the Agm is also grouped in the medial prefrontal cortex (Leonard 1969; Markowitsch and Pritzel 1981; Akhter et al. 2014). Therefore, it seems unlikely that the function of the centromedian thalamic nucleus in anthropoids and primates is analogous to that of the OPC in rats.

In summary, the present study has revealed a unique new thalamocortical pathway that possibly conveys the JCMS proprioceptive sensation via the OPC broadly (divergently) to the S1, S2, and GI, compared with the thalamocortical pathways from other intralaminar thalamic nuclei and sensory thalamic nuclei. Especially, this pathway is quite unique in comparison to the other pathway that conveys the JCMS proprioceptive sensation via the VPMcvm convergently to the dGIrvs2. The JCMS proprioceptive sensation via the OPC may be involved in both discriminative and integrative aspects of orofacial sensations.

Author contributions All authors read and approved the final manuscript. AY and YTa conceptualized the hypothesis, designed and supervised the experiments and directed the data analysis. YTs, YM, TH, and FS carried out the experiments and data analysis. TF and AO helped perform experiments and data analysis. AY, YTs, TF, MM, YCB, TY, and YTa finalized the figures and text.

Compliance with ethical standards

Conflict of interest The authors declare no potential conflicts of interest with respect to the authorship and/or publication of this article.

References

Akhter F, Haque T, Sato F, Kato T, Ohara H, Fujio T, Tsutsumi K, Uchino K, Ssssle BJ, Yoshida A (2014) Projections from the dorsal peduncular cortex to the trigeminal subnucleus caudalis (medullary dorsal horn) and other lower brainstem areas in rats. Neuroscience 266:23–37

Allen GV, Saper CB, Hurley KM, Cechetto DF (1991) Organization of visceral and limbic connections in the insular cortex of the rat. J Comp Neurol 311:1–16

Amassian VE, Berlin L (1958) Early cortical projection of group I afferents in forelimb muscle nerves of cat. J Physiol 143:61

Andersson SA, Landgren S, Wolsk D (1966) The thalamic relay and cortical projection of group I muscle afferents from the forelimb of the cat. J Physiol 183:576–591

Augustine JR (1985) The insular lobe in primates including humans. Neurol Res 7:2–10

Augustine JR (1996) Circuitry and functional aspects of the insular lobe in primates including humans. Brain Res Brain Res Rev 22:229–244

Benison AM, Rector DM, Barth DS (2007) Hemispheric mapping of secondary somatosensory cortex in the rat. J Neurophysiol 97:200–207

Benjamin RM, Akert K (1959) Cortical and thalamic areas involved in taste discrimination in the albino rat. J Comp Neurol 111:231–259

Benjamin RM, Pfaffmann C (1955) Cortical localization of taste in albino rat. J Neurophysiol 18:56–64

Berendse HW, Groenewegen HJ (1991) Restricted cortical termination fields of the midline and intralaminar thalamic nuclei in the rat. Neuroscience 42:73–102

Carvell GE, Simons DJ (1986) Somatotopic organization of the second somatosensory area (SII) in the cerebral cortex of the mouse. Somatosens Res 3:213–237

Cechetto DF, Saper CB (1987) Evidence for a viscerotopic sensory representation in the cortex and thalamus in the rat. J Comp Neurol 262:27–45

Chang Z, Haque T, Iida C, Seki S, Sato F, Kato T, Uchino K, Ono T, Nakamura M, Bae YC, Yoshida A (2009) Distribution of premotoneurons for jaw-closing and jaw-opening motor nucleus receiving contacts from axon terminals of primary somatosensory cortical neurons in rats. Brain Res 1275:43–53

Coggeshall RE, Lekan HA (1996) Methods for determining numbers of cells and synapses: a case for more uniform standards of review. J Comp Neurol 364:6–15

Donoghue JP, Parham C (1983) Afferent connections of the lateral agranular field of the rat motor cortex. J Comp Neurol 217:390–404

Donoghue JP, Wise SP (1982) The motor cortex of the rat: cytoarchitecture and microstimulation mapping. J Comp Neurol 212:76–88

Dostrovsky JO, Guilbaud G (1988) Noxious stimuli excite neurons in nucleus submedius of the normal and arthritic rat. Brain Res 460:269–280

Dostrovsky JO, Broton JG, Warma NK (1987) Functional properties of subnucleus caudalis lamina I neurons projecting to nucleus submedius. In: Schmidt RF, Schaible H-G, Vahle-Hinz C (eds) Fine afferent nerve fibers and pain. Springer, Germany

Dubner R, Sessle BJ, Storey AT (1978) The neural basis of oral and facial function. Plenum Press, New York

Fang PC, Stepniewska I, Kaas JH (2006) The thalamic connections of motor, premotor, and prefrontal areas of cortex in a prosimian primate (Otolemur garnetti). Neuroscience 143:987–1020

Felleman DJ, Wall JT, Cusick CG, Kaas JH (1983) The representation of the body surface in S-I of cats. J Neurosci 3:1648–1669

Francis JT, Xu S, Chapin JK (2008) Proprioceptive and cutaneous representations in the rat ventral posterolateral thalamus. J Neurophysiol 99:2291–2304

Friedman DP, Jones EG (1981) Thalamic input to areas 3a and 2 in monkeys. J Neurophysiol 45:59–85

Fujio T, Sato F, Tachibana Y, Kato T, Tomita A, Higashiyama K, Ono T, Maeda Y, Yoshida A (2016) Revisiting the supratrigeminal nucleus in the rat. Neuroscience 324:307–320

Furuta T, Deschênes M, Kaneko T (2011) Anisotropic distribution of thalamocortical boutons in barrels. J Neurosci 31:6432–6439

Gandevia SC, Macefield G (1989) Projection of low-threshold afferents from human intercostal muscles to the cerebral cortex. Respir Physiol 77:203–214

Gauriau C, Bernard JF (2004) Posterior triangular thalamic neurons convey nociceptive messages to the secondary somatosensory and insular cortices in the rat. J Neurosci 24:752–761

Groenewegen HJ, Galis-de Graaf Y, Smeets WJ (1999) Integration and segregation of limbic cortico-striatal loops at the thalamic

level: an experimental tracing study in rats. J Chem Neuroanat 16:167–185

Hamilton RB, Norgren R (1984) Central projections of gustatory nerves in the rat. J Comp Neurol 222:560–577

Hanamori T, Kunitake T, Kato K, Kannan H (1998a) Neurons in the posterior insular cortex are responsive to gustatory stimulation of the pharyngolarynx, baroreceptor and chemoreceptor stimulation, and tail pinch in rats. Brain Res 785:97–106

Hanamori T, Kunitake T, Kato K, Kannan H (1998b) Responses of neurons in the insular cortex to gustatory, visceral, and nociceptive stimuli in rats. J Neurophysiol 79:2535–2545

Haque T, Yamamoto S, Masuda Y, Kato T, Sato F, Uchino K, Oka A, Nakamura M, Takeda R, Ono T, Kogo M, Yoshida A (2010) Thalamic afferent and efferent connectivity to cerebral cortical areas with direct projections to identified subgroups of trigeminal premotoneurons in the rat. Brain Res 1346:69–82

Haque T, Akhter F, Kato T, Sato F, Takeda R, Higashiyama K, Moritani M, Bae YC, Sessle BJ, Yoshida A (2012) Somatotopic direct projections from orofacial areas of secondary somatosensory cortex to trigeminal sensory nuclear complex in rats. Neuroscience 219:214–233

Haroian AJ, Massopust LC, Young PA (1981) Cerebellothalamic projections in the rat: an autoradiographic and degeneration study. J Comp Neurol 197:217–236

Heath CJ, Hore J, Phillips CG (1976) Inputs from low threshold muscle and cutaneous afferents of hand and forearm to areas 3a and 3b of baboon's cerebral cortex. J Physiol (Lond) 257:199–227

Herbert H, Moga MM, Saper CB (1990) Connections of the parabrachial nucleus with the nucleus of the solitary tract and the medullary reticular formation in the rat. J Comp Neurol 293:540–580

Herkenham M (1980) Laminar organization of thalamic projections to the rat neocortex. Science 207:532–535

Hicks RR, Huerta MF (1991) Differential thalamic connectivity of rostral and caudal parts of cortical area Fr2 in rats. Brain Res 568:325–329

Iida C, Oka A, Moritani M, Kato T, Haque T, Sato F, Nakamura M, Uchino K, Seki S, Bae YC, Takada K, Yoshida A (2010) Corticofugal direct projections to primary afferent neurons in the trigeminal mesencephalic nucleus of rats. Neuroscience 169:1739–1757

Ikeda T, Terayama R, Jue S-S, Sugiyo S, Dubner R, Ren K (2003) Differential rostral projections of caudal brainstem neurons receiving trigeminal input after masseter inflammation. J Comp Neurol 465:220–233

Ikenoue E, Akhter F, Tsutsumi Y, Sato F, Ohara H, Uchino K, Furuta T, Tachibana Y, Yoshida A (2018) Transcortical descending pathways through granular insular cortex conveying orofacial proprioception. Brain Res 1687:11–19

Ito S (1992) Multiple projection of vagal non-myelinated afferents to the anterior insular cortex in rats. Neurosci Lett 148:151–154

Iwai H, Kuramoto E, Yamanaka A, Sonomura T, Uemura M, Goto T (2015) Ascending parabrachio-thalamo-striatal pathways: potential circuits for integration of gustatory and oral motor functions. Neuroscience 294:1–13

Iwamura Y, Tanaka M, Sakamoto M, Hikosaka O (1983) Functional subdivisions representing different finger regions in area 3 of the first somatosensory cortex of the conscious monkey. Exp Brain Res 51:315–326

Iwata K, Itoga H, Ikukawa A, Hanashima N, Sumino R (1985) Distribution and response characteristics of masseteric nerve-driven neurons in two separate cortical projection areas of cats. Brain Res 342:179–182

Jones EG (2007) The Thalamus. Cambridge University Press, Cambridge

Jones EG, Friedman DP (1982) Projection pattern of functional components of thalamic ventrobasal complex on monkey somatosensory cortex. J Neurophysiol 48:521–544

Jones EG, Friedman DP, Hendry SH (1982) Thalamic basis of place- and modality-specific columns in monkey somatosensory cortex: a correlative anatomical and physiological study. J Neurophysiol 48:545–568

Kosar E, Grill HJ, Norgren R (1986) Gustatory cortex in the rat II Thalamocortical projections. Brain Res 379:342–352

Krettek JE, Price JL (1977a) The cortical projections of the mediodorsal nucleus and adjacent thalamic nuclei in the rat. J Comp Neurol 171:157–192

Krettek JE, Price JL (1977b) Projections from the amygdaloid complex and adjacent olfactory structures to the entorhinal cortex and to the subiculum in the rat and cat. J Comp Neurol 172:723–752

Kriegsfeld LJ, Leak RK, Yackulic CB, LeSauter J, Silver R (2004) Organization of suprachiasmatic nucleus projections in Syrian hamsters (*Mesocricetus auratus*): an anterograde and retrograde analysis. J Comp Neurol 468:361–379

Lanciego LJ, Wouterlood FG (2011) A half century of experimental neuroanatomical tracing. Chem Neuroanat 42:157–383

Landgren S, Silfvenius H (1969) Projection to cerebral cortex of group I muscle afferents from the cat's hind limb. J Physiol 200:353–372

Leak RK, Moore RY (2001) Topographic organization of suprachiasmatic nucleus projection neurons. J Comp Neurol 433:312–334

Leonard CM (1969) The prefrontal cortex of the rat. I. Cortical projection of the mediodorsal nucleus. II. Efferent connections. Brain Res 12:321–343

Lund JP, Sessle BJ (1974) Oral-facial and jaw muscle afferent projections to neurons in cat frontal cortex. Exp Neurol 45:314–331

Lund JP, Richmond FJ, Touloumis C, Patry Y, Lamarre Y (1978) The distribution of Golgi tendon organs and muscle spindles in masseter and temporalis muscles of the cat. Neuroscience 3:259–270

Macefield G, Burke D, Gandevia SC (1989) The cortical distribution of muscle and cutaneous afferent projections from the human foot. Electroencephalogr Clin Neurophysiol 72:518–528

Maeda N, Kobashi M, Mitoh Y, Fujita M, Minagi S, Matsuo R (2014) Differential involvement of two cortical masticatory areas in submandibular salivary secretion in rats. Brain Res 1543:200–208

Maendly R, Rüegg DG, Wiesendanger M, Wiesendanger R, Lagowska J, Hess B (1981) Thalamic relay for group I muscle afferents of forelimb nerves in the monkey. J Neurophysiol 46:901–917

Markowitsch HJ, Pritzel M (1981) Prefrontal cortex of the guinea pig (*Cavia porcellus*) defined as cortical projection area of the thalamic mediodorsal nucleus. Brain Behav Evol 18:80–95

Mesulam MM, Mufson EJ (1982) Insula of the old world monkey. III: efferent cortical output and comments on function. J Comp Neurol 212:38–52

Moga MM, Saper CB (1994) Neuropeptide-immunoreactive neurons projecting to the paraventricular hypothalamic nucleus in the rat. J Comp Neurol 346:137–150

Nakashima M, Uemura M, Yasui K, Ozaki HS, Tabata S, Taen A (2000) An anterograde and retrograde tract-tracing study on the projections from the thalamic gustatory area in the rat: distribution of neurons projecting to the insular cortex and amygdaloid complex. Neurosci Res 36:297–309

Ogawa H, Wang XD (2002) Neurons in the cortical taste area receive nociceptive inputs from the whole body as well as the oral cavity in the rat. Neurosci Lett 322:87–90

Ohno S, Kuramoto E, Furuta T, Hioki H, Tanaka YR, Fujiyama F, Sonomura T, Uemura M, Sugiyama K, Kaneko T (2012) A morphological analysis of thalamocortical axon fibers of rat posterior thalamic nuclei: a single neuron tracing study with viral vectors. Cereb Cortex 22:2840–2857

Oscarsson O, Rosén I (1963) Projection to cerebral cortex of large muscle-spindle afferents in forelimb nerves of the cat. J Physiol 169:924–945

Oscarsson O, Rosén I (1966) Short-latency projections to the cat's cerebral cortex from skin and muscle afferents in the contralateral forelimb. J Physiol 182:164–184

Paxinos G, Watson C (1986) The rat brain in stereotaxic coordinates, 2nd edn. Academic Press, Sydney

Paxinos G, Watson C (1998) The rat brain in stereotaxic coordinates, 4th edn. Academic Press, Sydney

Paxinos G, Watson C (2014) The rat brain in stereotaxic coordinates, 7th edn. Academic Press, Sydney

Phillips CG, Powell TP, Wiesendanger M (1971) Projection from low-threshold muscle afferents of hand and forearm to area 3a of baboon's cortex. J Physiol 217:419–446

Pierret T, Lavallée P, Deschênes M (2000) Parallel streams for the relay of vibrissal information through thalamic barreloids. J Neurosci 20:7455–7462

Powell TP, Mountcastle VB (1959) Some aspects of the functional organization of the cortex of the postcentral gyrus of the monkey: a correlation of findings obtained in a single unit analysis with cytoarchitecture. Bull Johns Hopkins Hosp 105:133–162

Sadikot AF, Parent A, François C (1992) Efferent connections of the centromedian and parafascicular thalamic nuclei in the squirrel monkey: a PHA-L study of subcortical projections. J Comp Neurol 315:137–159

Sato F, Akhter F, Haque T, Kato T, Takeda R, Nagase Y, Sessle BJ, Yoshida A (2013) Projections from the insular cortex to pain-receptive trigeminal caudal subnucleus (medullary dorsal horn) and other lower brainstem areas in rats. Neuroscience 233:9–27

Sato F, Uemura Y, Kanno C, Tsutsumi Y, Tomita A, Oka A, Kato T, Uchino K, Murakami J, Haque T, Tachibana Y, Yoshida A (2017) Thalamo-insular pathway conveying orofacial muscle proprioception in the rat. Neuroscience 365:158–178

Sato F, Kado S, Tsutsumi Y, Tachibana Y, Ikenoue E, Furuta T, Uchino K, Bae YC, Uzawa N, Yoshida A (2020) Ascending projection of jaw-closing muscle-proprioception to the intralaminar thalamic nuclei in rats. Brain Res 1739:146830

Satoh Y, Ishizuka K, Murakami T (2007) Changes in cortically induced rhythmic jaw movements after lesioning of the red nucleus in rats. Brain Res 1165:60–70

Sirisko MA, Sessle BJ (1983) Corticobulbar projections and orofacial and muscle afferent inputs of neurons in primate sensorimotor cerebral cortex. Exp Neurol 82:716–720

Stepniewska I, Preuss TM, Kaas JH (2007) Thalamic connections of the dorsal and ventral premotor areas in New World owl monkeys. Neuroscience 147:727–745

Tomita A, Kato T, Sato F, Haque T, Oka A, Yamamoto M, Ono T, Bae YC, Maeda Y, Sessle BJ, Yoshida A (2012) Somatotopic direct projections from orofacial areas of primary somatosensory cortex to pons and medulla, especially to trigeminal sensory nuclear complex, in rats. Neuroscience 200:166–185

Tsutsumi Y, Tachibana Y, Sato F, Furuta T, Ohara H, Tomita A, Fujita M, Moritani M, Yoshida A (2018) Cortical and subcortical projections from granular insular cortex receiving orofacial proprioception. Neuroscience 388:317–329

Uemura Y, Haque T, Sato F, Tsutsumi Y, Ohara H, Oka A, Furuta T, Bae YC, Yamashiro T, Tachibana Y, Yoshida A (2020) Proprioceptive thalamus receiving forelimb and neck muscle spindle inputs via the external cuneate nucleus in the rat. Brain Struct Funct 225:2177–2192

Van der Werf YD, Witter MP, Groenewegen HJ (2002) The intralaminar and midline nuclei of the thalamus. Anatomical and functional evidence for participation in processes of arousal and awareness. Brain Res Brain Res Rev 39:107–140

Van Eden CG, Lamme VA, Uylings HB (1992) Heterotopic cortical afferents to the medial prefrontal cortex in the rat. A combined retrograde and anterograde tracer study. Eur J Neurosci 4:77–97

Waite PME (2004) Trigeminal sensory system. In: Paxinos G (ed) The rat nervous system, 3rd edn. Elsevier Academic Press, San Diego, pp 817–851

Waite PME, Tracey DJ (1985) Trigeminal sensory system. In: Paxinos G (ed) The rat nervous system, 2nd edn. Elsevier Academic Press, San Diego, pp 705–724

Welker C, Sinha MM (1972) Somatotopic organization of Sm II cerebral neocortex in albino rat. Brain Res 37:132–136

Wouterlood FG (2015) A survey of current Neuroanatomical tracing techniques. In: Arenkiel BR (ed) Neural tracing methods. Humana Press, New York, Tracing neurons and their connections, pp 1–49

Yamamoto T, Yuyama N, Kawamura Y (1981) Cortical neurons responding to tactile, thermal and taste stimulations of the rat's tongue. Brain Res 221:202–206

Yamamoto T, Matsuo R, Kiyomitsu Y, Kitamura R (1988) Sensory inputs from the oral region to the cerebral cortex in behaving rats: an analysis of unit responses in cortical somatosensory and taste areas during ingestive behavior. J Neurophysiol 60:1303–1321

Yamamoto T, Matsuo R, Kiyomitsu Y, Kitamura R (1989) Sensory and motor responses of trigeminal and reticular neurons during ingestive behavior in rats. Exp Brain Res 76:386–400

Yoshida A, Dostrovsky JO, Sessle BJ, Chiang CY (1991) Trigeminal projections to the nucleus submedius of the thalamus in the rat. J Comp Neurol 307:609–625

Yoshida A, Dostrovsky JO, Chiang CY (1992) The afferent and efferent connections of the nucleus submedius in the rat. J Comp Neurol 324:115–133

Yoshida A, Fukami H, Nagase Y, Appenteng K, Honma S, Zhang LF, Bae YC, Shigenaga Y (2001) Quantitative analysis of synaptic contacts made between functionally identified oralis neurons and trigeminal motoneurons in cats. J Neurosci 21:6298–6307

Yoshida A, Yamamoto M, Moritani M, Fukami H, Bae YC, Chang Z, Sugiyo S, Takemura M, Park KP, Shigenaga Y (2005) Bilateral projection of functionally characterized trigeminal oralis neurons to trigeminal motoneurons in cats. Brain Res 1036:208–212

Yoshida A, Taki I, Chang Z, Iida C, Haque T, Tomita A, Seki S, Yamamoto S, Masuda Y, Moritani M, Shigenaga Y (2009) Corticofugal projections to trigeminal motoneurons innervating antagonistic jaw muscles in rats as demonstrated by anterograde and retrograde tract-tracing. J Comp Neurol 514:368–386

Yoshida A, Fujio T, Sato F, Ali MS, Haque T, Ohara H, Moritani M, Kato T, Dostrovsky JO, Tachibana Y (2017) Orofacial proprioceptive thalamus of the rat. Brain Struct Funct 222:2655–2669

Zhang ZW, Deschênes M (1998) Projections to layer VI of the posteromedial barrel field in the rat: a reappraisal of the role of corticothalamic pathways. Cereb Cortex 8:428–436

Zhang GX, Sasamoto K (1990) Projections of two separate cortical areas for rhythmical jaw movements in the rat. Brain Res Bull 24:221–230